HHS Public Access

Author manuscript

Neurotox Res. Author manuscript; available in PMC 2019 October 01.

Published in final edited form as:

Neurotox Res. 2018 October ; 34(3): 584–596. doi:10.1007/s12640-018-9915-1.

Role of *Caenorhabditis elegans* AKT1/2 and SGK-1 in Manganese Toxicity

Tanara V. Peres[1,2], **Leticia Arantes**[1,3], **Mahfuzur R. Miah**[6], **Julia Bornhorst**[4], **Tanja Schwerdtle**[4], **Aaron B. Bowman**[5], **Rodrigo B. Leal**[7], and **Michael Aschner**[1]

[1]Department of Molecular Pharmacology, Albert Einstein College of Medicine, Bronx, NY, USA

[2]Programa de Pós-Graduação em Neurociências, Centro de Ciências Biológicas, Universidade Federal de Santa Catarina, Florianópolis, SC, Brazil

[3]Departamento de Bioquímica e Biologia Molecular, Centro de Ciências Naturais e Exatas, Universidade Federal de Santa Maria, Santa Maria, RS, Brazil

[4]Institute of Nutritional Science, University of Potsdam, Nuthetal, Germany

[5]Department of Pediatrics, Neurology and Biochemistry, Vanderbilt University Medical Center and Vanderbilt University, Nashville, TN, USA

[6]Department of Neuroscience, Albert Einstein College of Medicine, Bronx, NY, USA

[7]Departamento de Bioquímica, Programa de Pós-Graduação em Neurociências, Centro de Ciências Biológicas, Universidade Federal de Santa Catarina, Florianópolis, SC, Brazil

Abstract

Excessive levels of the essential metal manganese (Mn) may cause a syndrome similar to Parkinson's disease. The model organism *Caenorhabditis elegans* mimicks some of Mn effects in mammals, including dopaminergic neurodegeneration, oxidative stress and increased levels of Akt. The evolutionarily conserved insulin/insulin-like growth factor-1 signaling pathway (IIS) modulates worm longevity, metabolism and antioxidant responses by antagonizing the transcription factors DAF-16/FOXO and SKN-1/Nrf-2. AKT-1, AKT-2 and SGK-1 act upstream of these transcription factors. To study the role of these proteins in *C. elegans* response to Mn intoxication, wild-type N2 and loss-of-function mutants were exposed to Mn (2.5 to 100 mM) for 1 h at the L1 larval stage. Strains with loss-of-function in *akt-1*, *akt-2* and *sgk-1* had higher resistance to Mn compared to N2 in the survival test. All strains tested accumulated Mn similarly, as shown by ICP-MS. DAF-16 nuclear translocation was observed by fluorence microscopy in WT and loss-of-function strains exposed to Mn. qRT-PCR data indicate increased expression of γ-glutamyl cysteine synthetase (GCS-1) antioxidant enzyme in *akt-1* mutants. The expression of *sod-3* (superoxide dismutase homologue) was increased in the *akt-1* mutant worms, independent of Mn treatment. However, dopaminergic neurons degenerated even in the more resistant strains. Dopaminergic function was evaluated with the basal slowing response behavioral test and dopaminergic neuron integrity was evaluated using worms expressing green fluorescent protein

Corresponding author: Tanara V. Peres (orcid.org/0000-0003-0199-8653): tanara.peres-vieira@einstein.yu.edu or tanaravp@gmail.com, 1300 Morris Park Ave, Forchheimer 209, Bronx, NY, 10461, Telephone: 7184304047.

Conflict of Interest: The authors declare that they have no conflict of interest.

(GFP) under the dopamine transporter (DAT-1) promoter. These results suggest that AKT1/2 and SGK-1 play a role in *C. elegans* response to Mn intoxication. However, tissue-specific responses may occur in dopaminergic neurons, contributing to degeneration.

Keywords

Manganese; *C. elegans*; signaling pathways; DAF-16; Akt; SGK-1

Introduction

Manganese (Mn) is an essential metal that acts as a cofactor for several enzymes. However, individuals exposed to excessive Mn levels may display symptoms similar to Parkinson's disease (PD) and develop a syndrome called manganism (Aschner et al. 2009). The model organism *Caenorhabditis elegans* has proven invaluable in toxicological research of several agents, including Mn toxicity (Aitlhadj et al. 2011). It has been shown that Mn induces oxidative stress and reduced longevity in *C. elegans* (Au et al. 2009). Moreover, the nematode model has been instrumental in deciphering the role of dopamine (DA) and ROS generation in Mn-induced dopaminergic neurodegeneration (Benedetto et al. 2010). In mammals, oxidative stress represents a key effector mechanism of Mn-induced toxicity with specificity to dopaminergic (DAergic) neurons, reducing their viability and causing morphological changes (Farina et al. 2013; Guilarte 2013). Both effects are highly reproducible in *C. elegans.* Increased expression of Akt was also observed in worms exposed to Mn (Avila et al. 2012b).

The evolutionarily conserved insulin/insulin-like growth factor-1 signaling pathway (IIS) modulates worm longevity, metabolism and antioxidant responses. Klass (1983) was the first to screen *C. elegans* for long-lived mutants; the progression of IIS discovery was reviwed by Kenyon (2011). In *C. elegans* IIS is composed of DAF-2 (the only receptor similar to mammalian insulin-like growth factor 1, IGF-1, receptor) and is activated by insulin-like peptides, activating targets including Akt-1, Akt-2 and serum and glucocorticoid-regulated kinase (SGK-1) via AGE-1 (homologous of phosphatidyl inositol-3 kinase, PI3K) and phosphatidyl inositol-dependent kinase (PDK-1). This signaling pathway targets SKN-1 and DAF-16 transcription factors, which are phosphorylated by Akt 1/2 and SGK-1 at various sites and kept in the cytoplasm, decreasing the transcription of their target genes, including antioxidant response genes, which modulate redox status (Gatsi et al. 2014; Kenyon et al. 1993; Ogg et al. 1997; Paradis and Ruvkun 1998; Tullet et al. 2008). This signaling pathway was summarized in Figure 8. Mutations in *daf-2* (Kenyon et al. 1993) or in *age-1* (Friedman and Johnson 1988) cause retention in the dauer stage, fat storage and increased lifespan. In *C. elegans*' metabolism, glucose homeostasis control via alteration of key metabolic regulators activity, including glucose transporters and metabolic enzymes, is similar to the role of insulin in mammals (Hashmi et al. 2013; Paradis and Ruvkun 1998).

DAF-16 activates *sod-3* transcription, among other antioxidant response genes. SOD-3 is homologous to Mn-SOD and is located in the mitochondria (Honda and Honda 1999; Ogg et al. 1997). SKN-1 is important for digestive system development during early embryonic

stages, and is subsequently necessary for regulation of normal lifespan and stress resistance. In response to oxidative stress, SKN-1 translocates to the nucleus of intestinal cells, where it activates transcription of γ-glutamyl cysteine synthetase heavy chain [GCS(h)], glutathione synthetase and four isoforms of glutathione S-transferase (GST) (An and Blackwell 2003; Blackwell et al. 2015; Bowerman et al. 1992).

IIS regulation has been shown to promote resistance to various stressor agents, including metals. For example, the IIS components Akt-2 and SGK-1 have been shown to act pro-apoptotically in arsenite-exposed worms (Wang et al. 2014). Also, a loss-of-function mutation in *natc-1*, one of DAF-16 target genes, which encodes an N-acetyltransferase, promotes resistance to stress induced by excess zinc (Warnhoff et al. 2014). Furthermore, PDK-1 and Akt-1/2 were identified as metallothionein (MT) regulators, highlighting the role of IIS in *C. elegans* response to stressful stimuli such as cadmium exposure (Hall et al. 2017).

Using *C. elegans* as an *in vivo* model, the main goal of this study was to investigate the effects of AGC kinase family members *akt-1*, *akt-2* and *sgk-1* loss-of-function mutations on Mn-induced toxicity. These genes encode kinases that are key components of IIS and act upstream of DAF-16 and SKN-1. Therefore, we sought a better understanding of *C. elegans* conserved signaling pathways that mediate stress tolerance in response to Mn toxic levels, facilitating the identification of putative therapeutic targets. We found that strains with loss-of-function in *akt-1*, *akt-2* and *sgk-1* had higher resistance to Mn compared to N2 wild-type (WT) worms in the survival test, possibly due to antioxidant responses. However, we observed dopaminergic neurodegeneration even in the more resistant strains, suggesting tissue-specific responses may occur in dopaminergic neurons, leading to their degeneration.

Methods

Chemicals

Manganese chloride ($MnCl_2$), cholesterol, nicotinamide adenine dinucleotide phosphate (NADPH), glutathione (GSH), glutathione reductase (GR), 5,5′-dithiobis(2-nitrobenzoic acid) (DTNB), protease inhibitor, phosphatase inhibitor cocktails, polymerase chain reaction (PCR) primers and bovine serum albumin (BSA) were purchased from Sigma (St. Louis, MO, USA). TaqMan primers used for qRT-PCR analysis were obtained from Life Technologies (Carlsbad, CA, USA). Agar, peptone and agarose were purchased from BD (Franklin Lakes, NJ, USA). Trizol, SuperSignal West Pico chemiluminescent substrate and molecular weight marker for DNA were purchased from Thermo Fisher Scientific (Waltham, MA, USA). Protein molecular weight standard, Laemli buffer and precast acrylamide gels were from Bio Rad (Hercules, CA, USA). All other reagents were of analytical grade.

C. elegans culture and handling of the worms

The following strains were used: Bristol N2 WT, TJ356 [daf-16p::daf-16a/b::GFP + rol-6(su1006)] zIs356, MT15620 *cat-2*(*n4547*), the deletion mutants VC204 *akt-2(ok393)*, VC345 *sgk-1(ok538)*, RB759 *akt-1(ok525)*, and the gain-of-function (gof) GR1310 *akt-1(mg144)*. The worms were acquired from the *Caenorhabditis* Genetics Center (CGC -

University of Minnesota, Twin Cities, MN, USA). BY200 *Pdat-1::gfp* (vtIs1) was kindly provided by the Blakely laboratory, Vanderbilt University Medical Center.

Akt-2(ok393), sgk-1(ok538) or akt-1(ok525) were crossed with *Pdat-1::GFP* males for evaluation of dopaminergic neurons or with *Pdaf-16::DAF-16::gfp* for DAF-16 visualization. Selected worms were analyzed for the mutation of interest by PCR using standard methodology. F3 generation onward that expressed both GFP and the knockout were grown and used for the experiments.

Worms were maintained in standard culture conditions at 20°C in plastic petri dishes of 100 or 150 mm diameter containing agar 8P (3 g/L NaCl, 25 g/L agar; 20 g/L peptone; 1 mM $CaCl_2$, 5 mg/L cholesterol, 1 mM $MgSO_4$, 25 mM KPO_4) seeded with NA22 *Escherichia coli* (as food). During experiments worms were maintained on plates containing nematode growth medium (NGM: 3 g/L NaCl, 17 g/L agar, 2.5 g/L peptone, 1 mM $CaCl_2$, 5 mg/L cholesterol, 1 mM $MgSO_4$, 25 mM KPO_4 with 1,25 mL nystatin and 50 mg/L streptomycin sulfate) and *E. coli* OP50 strain was used as food (Brenner 1974). Synchronized populations at the L1 larval stage were obtained by isolation of embryos of gravid hermaphrodites using extraction solution (1% NaOCl, 0.25M NaOH). Eggs were isolated from cell debris by a 30% sucrose gradient (Sulston and Hodgkin 1988).

C. elegans exposure to Mn and survival assay

Acute treatments with $MnCl_2$ were conducted in populations of 2500 L1 worms based on the protocol described by Au et al. (2009), with modifications. Worms were exposed for 1 h to 2.5 – 100 mM $MnCl_2$ prepared in 85 mM NaCl to construct a dose-response curve. Treatments were performed in siliconized tubes with constant rotation at 20°C. The worms were then pelleted by centrifugation at 7000 rpm for 2 min and washed 3 times in 85 mM NaCl. On day 0, immediately after exposure to Mn, 40 to 60 worms were placed on 60 mm plates containing NGM and seeded with OP50 *E. coli*. Each condition was performed in triplicate. The surviving worms were counted 48 h after treatment. Results were expressed as a percentage live worms relative to day 0. Dose-response survival curves were constructed based on the percentage of worms alive 48 h post treatment plotted against the logarithmic scale of Mn concentrations by non-linear regression with a maximum of 100%, and enabled the calculation of lethal dose 50% (LD_{50}). All treatments were performed in triplicates and experiments were repeated independently at least three times. Subsequent treatments were performed with 10 or 50 mM $MnCl_2$, which are close to the LD_{50} calculated in this work.

Metal content

Mn, Fe, Cu, Zn, Ca and Mg levels were measured by inductively coupled plasma-mass spectrometry (ICP-MS) using the 8800 ICP-QQQ (Agilent, Santa Clara, CA). Briefly, 50,000 synchronized L1 worms were acutely treated with $MnCl_2$ for measurements 0 h post-treatment. Ten thousand L1 worms were treated for measurements 48 h post-treatment. Worms were maintained in NGM plates until processed for ICP-MS. Worms were washed five times in 85 mM NaCl to remove excess Mn from the medium, worms were re-suspended in 1 mL 85 mM NaCl supplemented with 1% protease inhibitor and sonicated. After sonication, an aliquot was taken for protein quantification using the bicinchoninic acid

(BCA) assay-kit (Thermo Scientific), the remaining solution was dried overnight at 60°C and incubated with the ashing mixture (65% HNO_3/30% H_2O_2 (1/1) (both from Merck) at 95°C for at least 12 h. After dilution of the ash with 2% HNO_3 including 10 μg/L Rh as internal standard the concentration of ^{56}Fe, ^{63}Cu, ^{66}Zn, ^{55}Mn, ^{44}Ca and ^{24}Mg was determined using ICP-MS with the instrumental parameters as previously described (Bornhorst et al. 2014).

Basal slowing response

This behavioral assay evaluates the functionality of the worms' dopaminergic system. The test was performed 48 h after Mn exposure and consists of washing the worms 3 times with S-basal buffer (100 mM NaCl, 5 mg/L cholesterol, 50 mM KPO_4, pH 6.0) to remove residual bacteria. Then five worms were placed on the center of a 60 mm plate containing NGM and OP50 bacteria spread in a ring shape. The ring had an outer diameter of approximately 3.5 cm and inner diameter of approximately 1 cm. Another five worms were placed on the center of a NGM plate without bacteria. The plates were prepared the day before and incubated overnight at 37°C. Two plates with and one without bacteria for each experimental group were used. After a period of 5 minutes of habituation, the number of bends that each worm performed in the anterior region of their body was counted by eye over a period of 20 s to determine its mobility rate. Upon reaching their food (bacteria) the worm has a mecanossensory response that reduces mobility. This response is known as basal slowing and depends on dopaminergic signaling. The three classes of dopaminergic neurons (CEP, ADE and PDE) participate in this response, mediating motor system control. The results were expressed as the difference (Δ) between the numbers of body bends in the plate with bacteria and without bacteria. A low Δ value means greater mobility on the food, indicating deficits in dopaminergic function. The *cat-2* mutant strain was used as a positive control in this test. This strain is deficient in tyrosine hydroxylase (CAT-2) homologue and has reduced levels of dopamine (Sawin et al. 2000).

Fluorescence microscopy for dopaminergic degeneration assay and DAF-16 localization

For observation of live worms, 30 worms were anesthetized with 30 μM levamisole hydrochloride and mounted on slides containing 2% agarose pads as previously described by Sulston (1976), with modifications. The worms were observed 2 h after exposure to Mn using a fluorescence microscope (Nikon Eclipse 80i, Nikon Corporation, Tokyo, Japan) equipped with a Xenon LS Lambda lamp (Sutter Instrument Company) and objective Nikon Plan Fluor 20x dry and Nikon Plan Apo 60x1.3 oil. Discontinuous GFP marking in the BY200 strain exposed to Mn is indicative of neurodegeneration (Benedetto et al. 2010). Each worm was scored for the absence (considered normal), or presence of any of the following morphological changes: puncta formation along dendritic processes, shrunk and/or lost soma, loss of dendrites (considered degenerate). Representative images of each condition are presented in Supplemental Figure 1. The results were expressed as percentage of degenerated worms compared to the total number of worms analyzed by treatment group (Bornhorst et al. 2014).

For DAF-16 visualitazion levamisole was not used as it may *per se* alter DAF-16 localization (Michaelson et al. 2010). Thirty TJ356 trangenic worms stably expressing a DAF-16::GFP

fusion protein as a reporter were mounted on slides containing 2% agarose pads. Worms were observed with the Nikon fluoresce microscope at 10 min or 1 h of Mn exposure to score the number of worms presenting nuclear, intermediate or cytoplasmic DAF-16::GFP (Lin et al. 2001).

Representative images for both assays were obtained with a PerkinElmer spinning disk confocal, 40 X objective (PerkinElmer, Waltham, MA, USA)

Glutathione (GSH) quantification

Approximately 50,000 worms were treated with control solution (85 mM NaCl) or $MnCl_2$ 10 or 50 mM for 1 h. Worms were washed with M9 buffer and sonicated in 100 μL extraction buffer (1% Triton X-100, 0.6% sulfosalicylic acid, 1% protease inhibitor, 5 mM EDTA in PBS). The resulting homogenate was centrifuged (10,000 rpm, 10 min, 4°C) and the supernatant was collected, discarding the cellular debris and undamaged worms. Protein content was determined with the BCA method using BSA as standard (Smith et al., 1985). To measure the total GSH level (oxidized and reduced) we used the method described by Rahman et al. (2006). This method is based on the reaction of thiol groups with DTNB to form a yellow anion 5-thio-2-nitrobenzoic acid (TNB) that can be measured at 412 nm. The samples were incubated in the presence of DTNB, GR and NADPH and the formation of TNB was measured for 2 min. The total concentration of GSH was determined using a standard curve of GSH. Results are expressed as nM GSH/mg protein.

qRT-PCR

To extract ribonucleic acid (RNA) 1 mL Trizol was added to the pellet of 50,000 worms after Mn exposure. The samples were frozen in liquid nitrogen and thawed at 37°C three times to break the worm's cuticle. Samples were centrifuged (14,000 rpm, 10 min, 4°C) and 200 μL chloroform was added for a complete extraction of proteins and other undesirable substances. After further centrifugation, the upper aqueous phase was transferred to RNAse free polypropylene tubes. Nucleic acids were precipitated by adding cold isopropanol, the tubes were inverted several times and incubated overnight at −20°C. After further centrifugation, the precipitate was washed by adding 300 μL 75% ethanol and then resuspended in 25 μL sterile RNase free water (Thermo Scientific, San Jose, CA, USA). Quantification and assessment of purity and integrity of the material were observed using NanoDrop 2000 Spectrophotometer (Thermo Scientific, San Jose, CA, USA). Only samples with 260/280 nm ratio between 1.8 and 2.0 and concentration above 200 ng/μL were used. cDNA synthesis was performed using the High-Capacity cDNA Reverse Transcription kit (Thermo Scientific, San Jose, CA, USA) with a standard amount of 1 μg of total RNA for each sample. Gene expression was determined using the following TaqMan probes (Life Technologies) *gst-4* (Ce02458730_g1), *gcs-1* (Ce02436726_g1), *skn-1* (Ce02407447_g1), *sod-3* (Ce02404515_g1), *afd-1* (Ce02414573_m1). *afd-1* [actin filament binding protein (AFaDin) homolog] was used as a housekeeping gene. We observed little variation in expression of this gene in previous experiments; therefore, we didn't use more than one housekeeping gene in this work. The amplification reaction was performed by initial denaturation at 50°C for 2 min followed by 95°C for 10 min and 40 thermal cycles of 95°C for 15 s and 60°C for 1 min. The real-time monitoring of PCR was performed in a

thermocycler CFX96 Real-time system with BioRad CFX manager software (BioRad, Hercules, CA, USA) by detecting the fluorescence levels of TaqMan reagent. All reactions of both target genes as endogenous control were performed in triplicate. The treshold Cycle (Ct) used for the analysis was the arithmetic average of the triplicates of the target and endogenous control genes. The relative expression of each gene was carried out by $2^{-\Delta\Delta Ct}$ method (Livak and Schmittgen 2001).

Western blotting

Phospho JNK or AMPK immunocontent was determined with the technique first described by Burnette (1981). Sample preparation was carried out as as follows: After treatments, 50,000 worms were homogenized by three cycles of freezing in liquid nitrogen and thawing at 37°C followed by sonication in RIPA buffer containing 1% protease inhibitor, 1% phosphatase inhibitor cocktail 2, 1% phosphatase inhibitor cocktail 3 (Sigma). Lysates were centrifuged (10,000 x g for 10 min, at 4°C) to eliminate cellular debris. Protein concentration was determined by BCA. Supernatants were diluted 1/1 (v/v) in Laemli buffer containing β-mercaptoethanol (final concentration 5%) and incubated for 5 min at 100°C. Thirty μg of total protein/track were separated by sodium dodecyl sulfate polyacrylamide gel electrophoresis (SDS-PAGE) using 10% precast gels (Bio Rad), followed by transfer to nitrocellulose membranes. After blocking with 5% BSA in tris buffered saline (TBS) for 1 hour, membranes were incubated overnight (4° C) with primary antibodies: Phospho AMP-activated protein Kinase (AMPK) (Cell signaling #2535, 1:1000), phospho c-Jun N-terminal Kinase (JNK) (Santa Cruz sc-12882, 1:2000), β-actin (Santa Cruz sc-1615, 1:10,000) or total JNK (Santa Cruz sc-571, 1:5000). Subsequently, membranes were incubated for 1 h at RT with HRP conjugate secondary antibodies against mouse (Invitrogen #31432, 1:10,000), goat (Thermo Scientific #31402, 1:10,000) or rabbit (Thermo Scientific #31460, 1:10,000). All steps were followed by three 5 minutes washes with TBS-T (TBS with the addition of Tween-20 0.1%, pH 7.5). Blots were developed with a chemiluminescent reaction (SuperSignal West Pico chemiluminescent substrate, Thermo Scientific). Bands were quantified using Image J (National Institutes of Health, Bethesda, MD, USA, http://imagej.nih.gov/ij/). Data were expressed as a fold change relative to the mean of controls of the same strain. All controls were normalized to a standard control sample applied to all gels to correct for variability that occurs during development of blots.

Statistical analysis

Results were expressed as mean ± S.E.M. and graphs and statistical analyzes were generated with GraphPad Prism 6.0 (GraphPad Software Inc., La Jolla, CA, USA). The different survival curves obtained for each mutant were analyzed by two-way analysis of variance (ANOVA) followed by *post hoc* Tukey's test. The results of basal slowing response, integrity of dopaminergic neurons, DAF-16 localization, GSH content, qRT-PCR and western blotting data were analyzed by two-way ANOVA followed by *post hoc* Tukey's test. DAF-16 localization values were plotted in stacked colums for better visualization of results, but only percent of worms with cytoplasmic DAF-16 were used for statistics. Results were considered significant when $p < 0.05$.

Results

Akt-1, *akt-2* and *sgk-1* null mutants are more resistant to Mn than WT

Survival was evaluated in L1 worms exposed to 2.5 – 100 mM Mn for 1 h. We observed a rightward shift in the dose-response curves for *akt-1*, *akt-2* and *sgk-1* null mutants and significant differences in LD_{50} values: 51.56, 50.31 and 48.76 mM Mn, respectively, compared to 15.58 mM Mn for WT N2 [F (4, 160) = 8.616, p<0.0001]. This indicates increased resistance to Mn. The Akt-1 gof mutant was not significantly different from WT N2 control (Figure 1).

Intraworm metal accumulation is analogous in all strains

All strains showed increased Mn accumulation immediately (0 h) after exposure to 50 mM Mn, and two-way ANOVA revealed no significant difference between the strains [F (4, 30) = 0.614, p = 0.65]. Unlike the other strains, *akt-1* null mutants' Mn levels exposed to 10 mM Mn was statistically indistinguishable from the controls (Figure 2A). Mn content remained elevated in worms treated with 50 mM Mn 48 h post-treatment (adult worms) without differences between the various strains [F (4, 30) = 0.615, p = 0.65] (Figure 2B). Ca levels were altered only in *sgk-1* null mutatnts [F (4, 30) = 3.755, p < 0.05] (Figure 2C). No significant alterations were observed in Mg, Fe, Cu or Zn levels (data not shown).

Antioxidant response in *akt-1*, *akt-2* and *sgk-1* null mutants exposed to Mn

The null mutants *akt-1(ok525)*, *akt-2(ok593)*, *sgk-1(ok538)* were crossed with *Pdaf-16::DAF-16::GFP* worms for *in vivo* visualization of DAF-16 localization by fluorescence microscopy. Worms were visualized within 10 min of Mn treatment and at the end of treatment (1 h). Mn treatment (50 mM) induced DAF-16 nuclear localization in WT and *sgk-1* mutants within the first 10 min of exposure (Figure 3D). Two-way ANOVA revealed a significant effect of dose [F (2, 42) = 10.79, p<0.001]. This effect was not observed after 1 h Mn (Figure 3E).

As described above, the signaling pathway PI3K/AKT antagonizes the action of SKN-1 and DAF- 16 transcription factors. Therefore we tested by qRT-PCR the relative levels of expression of *sod-3* as a target of DAF-16 and the transcription factor *skn-1* and its target genes, *gst-4* and *gcs-1*. mRNA was extracted from null mutants *akt-1(ok525)*, *akt-2(ok593)*, *sgk-1(ok538)* or *akt-1(mg144)* gof mutant at the end of 1 h Mn (10 or 50 mM) exposure. *Akt-1* null mutants showed an increase in the relative expression of *gcs-1* (Figure 4D) with significant effect of dose [F (2, 35) = 4.39; p <0.05], and strain [F (4, 35) = 5.98; p <0.001], but no dose x strain interaction (p> 0.05). *Akt-1* mutants showed an increase in the relative expression of *sod-3* independent of Mn exposure (Figure 4A) with significant effect of strain [F (4, 40) = 19.62; p <0.001] absent a concentration effect (p> 0.05), and no strain x dose interaction (p> 0.05). There was no significant difference in the expression of *gst-4* and *skn-1. Akt-1* gof, *akt-2* and *sgk-1* mutants didn't show significant alterations in mRNA levels (p> 0.05; Figure 4B, C).

GSH levels in WT N2 worms decreased in response to 50 mM Mn exposure for 1 h ($p < 0.05$). The null mutants *akt-1* and *akt-2* did not show this decrease in GSH levels compared to WT group [$F(4, 30) = 4.05$; $p < 0.01$] (Figure 4E).

Mn induces similar DAergic neurodegeneration in WT and *akt-1*, *akt-2* and *sgk-1* mutant worms

Thirty worms per experiment were observed under fluorescent microscopy and scored for DAergic neurodegeneration (puncta, shrunken soma, loss of soma or dendrites). Figure 5A represents worms with healthy neurons (scored as normal). Figure 5B shows worms with puncta (discontinuous marking of the dendrite, indicated by arrows). Figure 5C shows loss or cell body shrinkage (arrowhead) and loss of dendrites (asterisks). These worms were scored as degenerated. DAergic neurodegeneration was observed at the highest dose with a significant effect of dose [$F(2, 44) = 34.42$, $p<0.001$] and no difference between strains ($p>0.05$) (Figure 5).

When encountering food, *C. elegans* slow down their movement (body bends) in a response referred to as basal slowing response (BSR) (Sawin et al. 2000). This depends on the mechanossensory DAergic neurons present in the head. When DAergic signaling is impaired, BSR doesn't occur, such as in the *cat-2* mutant. We tested this behavior in WT N2 and mutant worms exposed to Mn by counting the number of body bends off-food and on-food, and calculating the difference (Δ) between the two conditions. *Cat-2* mutants were used as positive control. BSR impairment was observed in strains exposed to 50 mM Mn: WT N2 worms ($\Delta = 7.46 \pm 0.61$, $p < 0.05$), *akt-1* gain of function ($\Delta = 7.10 \pm 2.37$; $p < 0.05$), *akt-1* null ($\Delta = 6.36 \pm 1.58$, $p < 0.05$) and *akt-2* null ($\Delta = 6.12 \pm 0.83$; $p < 0.01$), compared to the WT control group ($\Delta = 11.53 \pm 0.15$). A significant effect of dose was present [$F(2, 41) = 9.55$; $p<0.001$] with no difference between strains ($p > 0.05$). The *sgk-1* null mutant did not display significant BSR impairment (Figure 6).

Increased phospho JNK in worms exposed to Mn

Phospho JNK immunocontent was increased in all four strains (Figure 7A – D). In N2 there was a 9.89 ± 0.63 fold increase in worms exposed to 10 mM Mn and 21.02 ± 2.21 fold increase in N2 exposed to 50 mM Mn [$F(2, 9)=56.80$, $p<0.001$]. In *akt-1*, *akt-2* and *sgk-1* there was 9.61 ± 2.17, [$F(2, 9)=12.56$, $p<0.01$], 11.29 ± 2.21, [$F(2, 9)=18.63$, $p<0.001$] and 8.03 ± 0.75, [$F(2, 9)=46.02$, $p<0.001$] fold increase in worms exposed to 50 mM Mn, respectively. No alteration in the mutant strains was observed at the lowest dose.

Phosphorylated AMPK levels were not altered in any of the strains tested ($p>0.05$) (Figure 7E–H).

Discussion

We used Akt or SGK-1 signaling deficient *C. elegans* mutants, seeking a better understanding of the role of these pathways in Mn toxicity. The worms were exposed to Mn at the L1 larval stage, the first stage of post-embryonic development and a period of neurogenesis (Altun and Hall 2011). Survival assays revealed that the worms deficient in Akt-1, Akt-2 or SGK-1 have greater resistance to Mn compared to the WT group. This

indicates that these proteins participate in the mechanism of Mn-induced toxicity in *C. elegans*. Interestingly, gof mutants (mg144 allele) were analogous to N2 worms, in viability, behavioral test and in antioxidant response. This implies that increased Akt-1 expression does not significantly alter its effect on the transcription factors SKN-1 and DAF-16, and does not worsen Mn toxicity.

Several studies have shown Akt activation in response to Mn, but the role this protein plays in the metal-induced toxicity mechanism remains elusive. Activation of Akt by phosphorylation at Ser473 occurs in immature rats' striatum in response to Mn exposure, independent of oxidative stress (Cordova et al. 2013; Cordova et al. 2012). Akt activation was observed in STHdh striatal cells exposed to Mn, its role in metal toxicity remaining unclear (Bryan et al. 2017; Williams et al. 2010). Furthermore, exposure to Mn induced increase in Akt levels in *C. elegans* (Avila et al. 2012b). Akt also plays a role in Mn-induced precocious pubertal development by activating mTOR and target genes critical for the onset of puberty. Furthermore, Mn stimulated a dose-dependent release of hypothalamic IGF-1 *in vitro* and induced increase in the hypothalamic expression of p-IGF-1R (Srivastava et al. 2016).

The activation of Akt has been classically related to neuroprotection, reviewed by Brunet et al. (2001). However, the results obtained in this study using *C. elegans* suggest that Akt might participate, at least in part, in the mechanism of Mn toxicity. This participation cannot be directly related to cell death pathways activation, but may occur by antagonizing DAF-16 and SKN-1, and thus contribute to oxidative stress.

It has been suggested that inhibiting PI3K reduces Mn accumulation *in vitro* (Bryan et al. 2017); however in the worms tested herein, we did not observe differences in Mn content across strains. Future experiments should be planned to test *age-1* (PI3K homologue in worms) mutants to confirm if a similar effect is inherent to the worms.

The role of DAF-16 in Mn toxicity has been demonstrated before. The antioxidant compound diethyl-2-phenyl-2-telurofenil vinyl phosphonate (DPTVP) protects against oxidative stress caused by Mn by a mechanism that involves the translocation of DAF-16 to the nucleus (Avila et al. 2012a). A similar effect was obtained with the seleno-xilofuranoside compound and its tellurium analogue, noting increased SOD-3 levels and reduction in the toxic effects associated with Mn exposure in worms (Wollenhaupt et al. 2014). Therefore, the absence of Akt-1/2 or SGK-1 in mutant worms may relieve the inhibition of DAF-16, and thereby increase worm resistance to Mn. It's plausible DAF-16 is not the only target of these kinases with altered activity in mutants. We visualized DAF-16 nuclear translocation in WT worms, within 10 min of Mn exposure; however this was not associated with increased resistance to Mn.

Daf-2 mutant worms have higher SOD-3 levels compared to WT, even in the absence of a stressful stimulus, a phenotype associated with increased resistance to oxidative stress and longevity (Honda and Honda 1999). Our qRT-PCR results indicate that deficiency in Akt-1, a DAF-2 downstream target, has a similar phenotype and this could partly explain its greater

resistance to Mn. The same was not observed for *akt-2* or *sgk-1* mutants, suggesting that Akt-1 acts more critically in antioxidant enzymes production than the other two kinases.

Interestingly, not all DAF-16 targets were increased in control *akt-1* worms, and not all mutant worms displayed DAF-16 nuclear localization. This could be due to other factors that control DAF-16 shuttling. Furthermore, since we did not use double mutants, when one kinase was absent, the other may still phosphorylate DAF-16. Nonetheless, it was still possible to observe differences in worm survival and antioxidant response.

SKN-1 is a known target of IIS and it's associated with oxidative stress resistance. *Gcs-1* is one of its targets and it encodes a limiting enzyme for the synthesis of GSH, displaying increased expression in oxidative stress conditions (An and Blackwell 2003). We failed to observe an increase in its expression in N2 worms exposed to Mn. We observed, however, a decrease in total GSH levels in N2 worms exposed to 50 mM Mn, suggesting the presence of oxidative stress and consumption of GSH in ROS detoxification. WT worms were unable to produce sufficient GSH to maintain analogous levels to controls, unlike mutant worms, which did not display decreased GSH levels. *Akt-1* null mutants, on the other hand had increased content of *gcs-1* mRNA when exposed to 50 mM Mn. This mutant may have increased SKN-1 activity compared to the other strains, thus generating a resistance phenotype to oxidative stress.

Although the null mutants have higher resistance to Mn, DAergic neurodegeneration in these worms was similar to WT as demonstrated by basal slowing test and analysis of DAergic neurons expressing GFP. The *akt-1* gain of function mutants also showed a similar DAergic deficiency in basal slowing response. This indicates that Akt signaling may not be as important for the pathway that leads to the death of these DAergic neurons induced by Mn. Akt-1 and Akt-2 are expressed in most neurons of the head region, pharynx, hypodermis and intestine and Akt-1 appears to be more abundant than Akt-2 (Paradis and Ruvkun 1998). The greater viability of mutant worms exposed to Mn may be due to the antioxidant response present in the intestine, ensuring worm survival, but without protecting dopaminergic neurons, since Mn accumulates preferentially in worm intestine (Brinkhaus et al. 2014). *C. elegans* is able to survive even with its neuronal function severely (but not fully) impaired (Rand and Nonet 1997).

The *sgk-1* mutants exposed to Mn did not show deficiency in basal slowing response. The SGK-1 enzyme acts in parallel to Akt-1/2, but its role is distinguished from the other two kinases. SGK-1 is involved in post-embryonic development, stress resistance and longevity in a different way than Akt-1/2 (Chen et al. 2013; Gatsi et al. 2014; Hertweck et al. 2004). Chen et al. (2013) propose SGK-1 does not retain DAF-16 in cytoplasm, and acts through a different pathway to influence worm lifespan. Because behavioral was assessed 48 h post exposure and neurons analysed 2 h, future experiments should investigate the viability of dopaminergic neurons in *sgk-1* mutant strain to confirm if they remain healthy 48 h after Mn exposure.

Our data indicate a distinct response occurs in DAergic neurons and non-neuronal tissues of worms exposed to Mn. It has been demonstrated that IIS displays tissue-specific response in

neuronal and non-neuronal tissues, due to neuron-specific DAF-16 targets (Kaletsky et al. 2016), therefore AKT/SGK, which act upstream of DAF-16, induced different outcomes in various tissues. Mn exposure induces oxidative stress by extracelullar interaction with DA via NADPH oxidase-mediate mechanism and induces DAergic degeneration, as described by Benedetto et al. (2010). Therefore, it is plausible that oxidative stress-dependent signaling mechanisms induce DAergic degeneration in worms. This would be independent of AKT/SGK expression, and because both WT and mutants accumulate Mn in a similar way, we expect their DAergic neurons to be exposed to similar ROS levels and degenerate in an analogous fashion. Although the mutants display increased antioxidant response and survival, it seems oxidating species still damage their neurons, which reinforces the notion that the uptake of oxidizing agents needs to be addressed in order to prevent DAergic degeneration. Further studies should investigate the role of antioxidant stress response specific to DAergic neurons.

The JNK pathway is activated by various stressor signals, including oxidative stress, and acts proaptotically in neurons (Yang et al. 1997; Zeke et al. 2016). Accordingly, we observed increased JNK phosphorylation in worms exposed to Mn, which could be in response to oxidative stress produced by Mn interaction with DA. Furthermore, JNK knockdown has been shown to improve DAergic neurons viability in Mn exposed worms (Settivari et al. 2013).

AAK-2/AMPK is an important IIS target in aging-related studies in *C. elegans* (Mair et al. 2011; Tullet et al. 2014). AMPK is activated by AMP and stimulates glucose uptake to restore ATP levels. AAK-2/AMPK influences lifespan in parallel to DAF-2, but in a DAF-16 independent manner (Apfeld et al. 2004; Moreno-Arriola et al. 2016). No alterations were observed in AMPK phosphorylation in WT worms exposed to Mn. Our results indicate AMPK is unlikely to participate in resistance to Mn in mutant worms.

Heat-shock factor 1 (HSF-1) is another transcription factor downstream of DAF-2 signalling. HSF-1 is active in multiple tissues and modulates lifespan parallel to IIS (Hsu et al. 2003; Morley and Morimoto 2004). Lack of *hsf-1* did not alter Mn lethality or oxidative stress, while the absence of *hsp-70* gene lead to increased sensitivity to Mn-induced neurotoxicity (Avila et al. 2016). Further insvestigation on the role of HSPs on Mn neurotoxicity could clarify the tissue specifity observed in our study.

Interestingly, we found alterations in Ca levels only in *sgk-1* mutants exposed to Mn. Intracelular Ca regulates SGK-1 activity in cell models (Brickley et al. 2013), but it is not clear if there is a feedback response to loss-of-function *sgk-1* to increase Ca in worms. Our results indicate a role for this kinase in regulating Ca levels in worms. Wether this may also affect resistance to Mn exposure should be investigated in future studies. Basal Ca levels are higher at 48 h than in L1 worms. This is consistent with the need for Ca during fertilization (Singaravelu and Singson 2013).

Increased resistance to Mn in Akt-1/2 and SGK-1 deficient worms may be in part related to increased antioxidant response, resultant from DAF-16 and SKN-1 activity in the absence of these kinases (Figure 8). We did not observe protection of DAergic neurons in these mutants,

suggesting tissue-specific responses to Mn toxicity. This indicates Akt and SGK-1 as potential target for therapies against Mn toxicity, while demonstrating the importance of tissue-specific therapeutic approaches.

Supplementary Material

Refer to Web version on PubMed Central for supplementary material.

Acknowledgments

TVP received a fellowship from Coordenação de Aperfeiçoamento de Pessoal de Nível Superior (CAPES) Foundation, Ministry of Education of Brazil, (Proc. #0407/13-5) during part of this project. LA received a fellowship from Conselho Nacional de Desenvolvimento Científico e Tecnológico (CNPq, 202662/2014-4 - SWE). MA and ABB were supported by National Institute of Healt (NIH) R01 ES10563. MA was also supported by R01 ES07331 and R01 ES020852. We thank the “Deutsche Forschungsgemeinschaft” (DFG) further for the financial support of Schw 903/9-1 and BO 4103/2-1. Images were obtained at the Analytical Imaging Facility of the Albert Einstein College of Medicine [NCI cancer center support grant (P30CA013330)]. Some strains were provided by the CGC, which is funded by NIH Office of Research Infrastructure Programs (P40 OD010440). Funding agencies had no role in the study design, data collection and analysis, decision to publish, or preparation of the manuscript.

References

Aitlhadj L, et al. 2011; Environmental exposure, obesity and Parkinson’s disease: lessons from fat and old worms. Environ Health Perspect. 119:20–28. [PubMed: 20797931]

Altun ZF, Hall DH. 2011Nervous system, general description. WormAtlas. Accessed September 17 2016

An JH, Blackwell TK. 2003; SKN-1 links C. elegans mesendodermal specification to a conserved oxidative stress response. Genes Dev. 17:1882–1893. DOI: 10.1101/gad.1107803 [PubMed: 12869585]

Apfeld J, O’Connor G, McDonagh T, DiStefano PS, Curtis R. 2004; The AMP-activated protein kinase AAK-2 links energy levels and insulin-like signals to lifespan in C. elegans Genes Dev. 18:3004–3009. DOI: 10.1101/gad.1255404 [PubMed: 15574588]

Aschner M, Erikson K, Hernández E, Tjalkens R. 2009; Manganese and its Role in Parkinson’s Disease: From Transport to Neuropathology. NeuroMol Med. 11:252–266. DOI: 10.1007/s12017-009-8083-0

Au C, Benedetto A, Anderson J, Labrousse A, Erikson K, Ewbank JJ, Aschner M. 2009; SMF-1, SMF-2 and SMF-3 DMT1 Orthologues Regulate and Are Regulated Differentially by Manganese Levels in *C. elegans*. PLoS One. 4:e7792.doi: 10.1371/journal.pone.0007792 [PubMed: 19924247]

Avila DS, Benedetto A, Au C, Bornhorst J, Aschner M. 2016; Involvement of heat shock proteins on Mn-induced toxicity in Caenorhabditis elegans. BMC Pharmacology and Toxicology. 17:54.doi: 10.1186/s40360-016-0097-2 [PubMed: 27802836]

Avila DS, et al. 2012a; Organotellurium and organoselenium compounds attenuate Mn-induced toxicity in Caenorhabditis elegans by preventing oxidative stress. Free Radical Biol Med. 52:1903–1910. DOI: 10.1016/j.freeradbiomed.2012.02.044 [PubMed: 22406322]

Avila DS, Somlyai G, Somlyai I, Aschner M. 2012b; Anti-aging effects of deuterium depletion on Mn-induced toxicity in a C. elegans model. Toxicol Lett. 211:319–324. DOI: 10.1016/j.toxlet.2012.04.014 [PubMed: 22561170]

Benedetto A, Au C, Avila DS, Milatovic D, Aschner M. 2010; Extracellular dopamine potentiates Mn-induced oxidative stress, lifespan reduction, and dopaminergic neurodegeneration in a BLI-3-dependent manner in *Caenorhabditis elegans*. PLoS Genet. 6(8)doi: 10.1371/journal.pgen.1001084

Blackwell TK, Steinbaugh MJ, Hourihan JM, Ewald CY, Isik M. 2015; SKN-1/Nrf, stress responses, and aging in Caenorhabditis elegans. Free Radic Biol Med. 88:290–301. DOI: 10.1016/j.freeradbiomed.2015.06.008 [PubMed: 26232625]

Bornhorst J, et al. 2014; The effects of pdr1, djr1.1 and pink1 loss in manganese-induced toxicity and the role of [small alpha]-synuclein in C. elegans Metallomics. 6:476–490. DOI: 10.1039/C3MT00325F [PubMed: 24452053]

Bowerman B, Eaton BA, Priess JR. 1992; skn-1, a maternally expressed gene required to specify the fate of ventral blastomeres in the early C. elegans embryo. Cell. 68:1061–1075. [PubMed: 1547503]

Brenner S. 1974; The genetics of Caenorhabditis elegans. Genetics. 77:71–94. [PubMed: 4366476]

Brickley DR, et al. 2013; Serum- and Glucocorticoid-induced Protein Kinase 1 (SGK1) Is Regulated by Store-operated Ca2+ Entry and Mediates Cytoprotection against Necrotic Cell Death. J Biol Chem. 288:32708–32719. DOI: 10.1074/jbc.M113.507210 [PubMed: 24043625]

Brinkhaus SG, et al. 2014; Elemental bioimaging of manganese uptake in C. elegans Metallomics. 6:617–621. DOI: 10.1039/C3MT00334E [PubMed: 24481269]

Brunet A, Datta SR, Greenberg ME. 2001; Transcription-dependent and -independent control of neuronal survival by the PI3K-Akt signaling pathway. Curr Opin Neurobiol. 11:297–305. [PubMed: 11399427]

Bryan MR, et al. 2017; Phosphatidylinositol 3 kinase (PI3K) modulates manganese homeostasis and manganese-induced cell signaling in a murine striatal cell line. Neurotoxicology. doi: 10.1016/j.neuro.2017.07.026

Burnette WN. 1981; "Western Blotting": Electrophoretic transfer of proteins from sodium dodecyl sulfate-polyacrylamide gels to unmodified nitrocellulose and radiographic detection with antibody and radioiodinated protein A. Anal Biochem. 112:195–203. DOI: 10.1016/0003-2697(81)90281-5 [PubMed: 6266278]

Chen AT, Guo C, Dumas KJ, Ashrafi K, Hu PJ. 2013; Effects of Caenorhabditis elegans sgk-1 mutations on lifespan, stress resistance, and DAF-16/FoxO regulation. Aging Cell. 12:932–940. DOI: 10.1111/acel.12120 [PubMed: 23786484]

Cordova F, et al. 2013; Manganese-exposed developing rats display motor deficits and striatal oxidative stress that are reversed by Trolox. Arch Toxicol. :1–14. DOI: 10.1007/s00204-013-1017-5

Cordova FM, et al. 2012; In Vivo Manganese Exposure Modulates Erk, Akt and Darpp-32 in the Striatum of Developing Rats, and Impairs Their Motor Function. PLoS One. 7:e33057.doi: 10.1371/journal.pone.0033057 [PubMed: 22427945]

Farina M, Avila DS, da Rocha JB, Aschner M. 2013; Metals, oxidative stress and neurodegeneration: a focus on iron, manganese and mercury. Neurochem Int. 62:575–594. DOI: 10.1016/j.neuint.2012.12.006 [PubMed: 23266600]

Friedman DB, Johnson TE. 1988; A mutation in the age-1 gene in Caenorhabditis elegans lengthens life and reduces hermaphrodite fertility. Genetics. 118:75–86. [PubMed: 8608934]

Gatsi R, Schulze B, Rodriguez-Palero MJ, Hernando-Rodriguez B, Baumeister R, Artal-Sanz M. 2014; Prohibitin-Mediated Lifespan and Mitochondrial Stress Implicate SGK-1, Insulin/IGF and mTORC2 in C. elegans PLoS One. 9:e107671.doi: 10.1371/journal.pone.0107671 [PubMed: 25265021]

Guilarte TR. 2013; Manganese neurotoxicity: new perspectives from behavioral, neuroimaging, and neuropathological studies in humans and non-human primates. Frontiers in aging neuroscience. 5:23.doi: 10.3389/fnagi.2013.00023 [PubMed: 23805100]

Hall JA, McElwee MK, Freedman JH. 2017; Identification of ATF-7 and the insulin signaling pathway in the regulation of metallothionein in C. elegans suggests roles in aging and reactive oxygen species. PLoS One. 12:e0177432.doi: 10.1371/journal.pone.0177432 [PubMed: 28632756]

Hashmi S, Wang Y, Parhar RS, Collison KS, Conca W, Al-Mohanna F, Gaugler R. 2013; A C. elegans model to study human metabolic regulation. Nutrition & metabolism. 10:31.doi: 10.1186/1743-7075-10-31 [PubMed: 23557393]

Hertweck M, Göbel C, Baumeister R. 2004; C. elegans SGK-1 Is the Critical Component in the Akt/PKB Kinase Complex to Control Stress Response and Life Span. Dev Cell. 6:577–588. DOI: 10.1016/S1534-5807(04)00095-4 [PubMed: 15068796]

Honda Y, Honda S. 1999; The daf-2 gene network for longevity regulates oxidative stress resistance and Mn-superoxide dismutase gene expression in Caenorhabditis elegans. The FASEB Journal. 13:1385–1393. [PubMed: 10428762]

Hsu AL, Murphy CT, Kenyon C. 2003; Regulation of aging and age-related disease by DAF-16 and heat-shock factor. Science. 300:1142–1145. DOI: 10.1126/science.1083701 [PubMed: 12750521]

Kaletsky R, Lakhina V, Arey R, Williams A, Landis J, Ashraf J, Murphy CT. 2016; The C. elegans adult neuronal IIS/FOXO transcriptome reveals adult phenotype regulators. Nature. 529:92–96. DOI: 10.1038/nature16483 [PubMed: 26675724]

Kenyon C. 2011; The first long-lived mutants: discovery of the insulin/IGF-1 pathway for ageing. Philos Trans R Soc Lond B Biol Sci. 366:9–16. DOI: 10.1098/rstb.2010.0276 [PubMed: 21115525]

Kenyon C, Chang J, Gensch E, Rudner A, Tabtiang R. 1993; A C. elegans mutant that lives twice as long as wild type. Nature. 366:461.doi: 10.1038/366461a0 [PubMed: 8247153]

Klass MR. 1983; A method for the isolation of longevity mutants in the nematode Caenorhabditis elegans and initial results. Mech Ageing Dev. 22:279–286. [PubMed: 6632998]

Lin K, Hsin H, Libina N, Kenyon C. 2001; Regulation of the Caenorhabditis elegans longevity protein DAF-16 by insulin/IGF-1 and germline signaling. Nat Genet. 28:139–145. DOI: 10.1038/88850 [PubMed: 11381260]

Livak KJ, Schmittgen TD. 2001; Analysis of Relative Gene Expression Data Using Real- Time Quantitative PCR and the 2−ΔΔCT Method. Methods. 25:402–408. DOI: 10.1006/meth.2001.1262 [PubMed: 11846609]

Mair W, Morantte I, Rodrigues APC, Manning G, Montminy M, Shaw RJ, Dillin A. 2011; Lifespan extension induced by AMPK and calcineurin is mediated by CRTC-1 and CREB. Nature. 470:404-U179.doi: 10.1038/nature09706 [PubMed: 21331044]

Michaelson D, Korta DZ, Capua Y, Hubbard EJ. 2010; Insulin signaling promotes germline proliferation in C. elegans Development. 137:671–680. DOI: 10.1242/dev.042523 [PubMed: 20110332]

Moreno-Arriola E, El Hafidi M, Ortega-Cuellar D, Carvajal K. 2016; AMP-Activated Protein Kinase Regulates Oxidative Metabolism in Caenorhabditis elegans through the NHR-49 and MDT-15 Transcriptional Regulators. PLoS One. 11:e0148089.doi: 10.1371/journal.pone.0148089 [PubMed: 26824904]

Morley JF, Morimoto RI. 2004; Regulation of longevity in Caenorhabditis elegans by heat shock factor and molecular chaperones. Mol Biol Cell. 15:657–664. DOI: 10.1091/mbc.E03-07-0532 [PubMed: 14668486]

Ogg S, Paradis S, Gottlieb S, Patterson GI, Lee L, Tissenbaum HA, Ruvkun G. 1997; The Fork head transcription factor DAF-16 transduces insulin-like metabolic and longevity signals in C. elegans Nature. 389:994–999. DOI: 10.1038/40194

Paradis S, Ruvkun G. 1998; Caenorhabditis elegans Akt/PKB transduces insulin receptor-like signals from AGE-1 PI3 kinase to the DAF-16 transcription factor. Genes Dev. 12:2488–2498. [PubMed: 9716402]

Rand, JB, Nonet, ML. Components Regulating Neurotransmitter Release in all Neurons. In: Riddle, DL, Blumenthal, T, Meyer, BJ, Priess, JR, Hutchinson, F, editorsC. elegans II. 1997.

Sawin ER, Ranganathan R, Horvitz HR. 2000; C. elegans Locomotory Rate Is Modulated by the Environment through a Dopaminergic Pathway and by Experience through a Serotonergic Pathway. Neuron. 26:619–631. DOI: 10.1016/S0896-6273(00)81199-X [PubMed: 10896158]

Settivari R, VanDuyn N, LeVora J, Nass R. 2013; The Nrf2/SKN-1-dependent glutathione S-transferase π homologue GST-1 inhibits dopamine neuron degeneration in a Caenorhabditis elegans model of manganism. NeuroToxicology. 38:51–60. DOI: 10.1016/j.neuro.2013.05.014 [PubMed: 23721876]

Singaravelu G, Singson A. 2013; Calcium signaling surrounding fertilization in the nematode Caenorhabditis elegans. Cell Calcium. 53:2–9. DOI: 10.1016/j.ceca.2012.11.009 [PubMed: 23218668]

Srivastava VK, Hiney JK, Dees WL. 2016; Manganese-Stimulated Kisspeptin Is Mediated by the IGF-1/Akt/Mammalian Target of Rapamycin Pathway in the Prepubertal Female Rat. Endocrinology. 157:3233–3241. DOI: 10.1210/en.2016-1090 [PubMed: 27309941]

Sulston, J; Hodgkin, J. [Date accessed: 16 Mar. 2018] Methods; Cold Spring Harbor Monograph Archive, North America. 1988. 17Available at: https://cshmonographs.org/index.php/monographs/article/view/5032

Sulston JE. 1976; Post-embryonic development in the ventral cord of Caenorhabditis elegans. Philos Trans R Soc Lond B Biol Sci. 275:287–297. [PubMed: 8804]

Tullet JM, et al. 2008; Direct inhibition of the longevity-promoting factor SKN-1 by insulin-like signaling in C. elegans Cell. 132:1025–1038. DOI: 10.1016/j.cell.2008.01.030 [PubMed: 18358814]

Tullet JMA, et al. 2014; DAF-16/FoxO Directly Regulates an Atypical AMP-Activated Protein Kinase Gamma Isoform to Mediate the Effects of Insulin/IGF-1 Signaling on Aging in *Caenorhabditis elegans*. PLoS Genet. 10:e1004109.doi: 10.1371/journal.pgen.1004109 [PubMed: 24516399]

Wang S, Teng X, Wang Y, Yu HQ, Luo X, Xu A, Wu L. 2014; Molecular control of arsenite-induced apoptosis in Caenorhabditis elegans: roles of insulin-like growth factor-1 signaling pathway. Chemosphere. 112:248–255. DOI: 10.1016/j.chemosphere.2014.04.021 [PubMed: 25048913]

Warnhoff K, et al. 2014; The DAF-16 FOXO transcription factor regulates natc-1 to modulate stress resistance in Caenorhabditis elegans, linking insulin/IGF-1 signaling to protein N-terminal acetylation. PLoS Genet. 10:e1004703.doi: 10.1371/journal.pgen.1004703 [PubMed: 25330323]

Williams BB, et al. 2010; Disease-toxicant screen reveals a neuroprotective interaction between Huntington's disease and manganese exposure. J Neurochem. 112:227–237. DOI: 10.1111/j.1471-4159.2009.06445.x [PubMed: 19845833]

Wollenhaupt SGN, et al. 2014; Seleno- and Telluro-xylofuranosides attenuate Mn-induced toxicity in C. elegans via the DAF-16/FOXO pathway. Food Chem Toxicol. 64:192–199. DOI: 10.1016/j.fct.2013.11.030 [PubMed: 24296137]

Yang DD, et al. 1997; Absence of excitotoxicity-induced apoptosis in the hippocampus of mice lacking the Jnk3 gene. Nature. 389:865–870. DOI: 10.1038/39899 [PubMed: 9349820]

Zeke A, Misheva M, Remenyi A, Bogoyevitch MA. 2016; JNK Signaling: Regulation and Functions Based on Complex Protein-Protein Partnerships Microbiol. Mol Biol Rev. 80:793–835. DOI: 10.1128/MMBR.00043-14

A

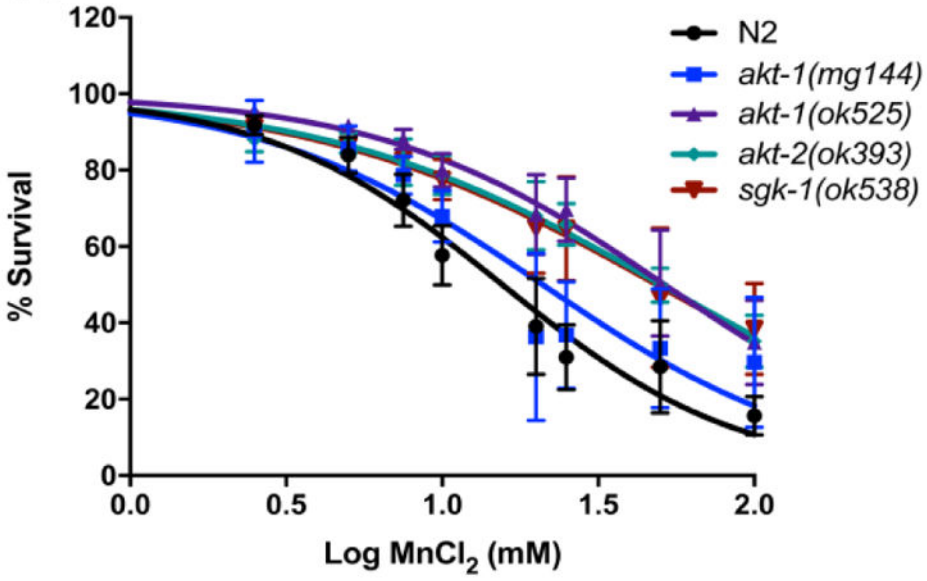

B

Strain	LD_{50} (mM)
N2	15.58
akt-1(ok525)	51.56***
akt-2(ok393)	50.31***
sgk-1(ok538)	48.76**
akt-1(mg144)	20.99

Fig. 1.

C. elegans (L1) survival after exposure to Mn (2.5–100 mM) for 1 h. Controls were incubated with 85 mM NaCl. The number of surviving worms was determined 48 h after treatment in N2 (wild-type, WT) or null mutants *akt-1(ok525), akt-2(ok593), sgk-1(ok538)* or gain-of-function mutant *akt-1(mg144)*. (A) Data represent the percentage of surviving worms relative to day 0 and are expressed as mean ± S.E.M. of 3 to 6 experiments and is plotted against the logarithmic scale of Mn concentrations. (B) Lethal dose 50% (LD50) was calculated by non-linear regression. ** P <0.01 *** p <0.001 compared with WT group, two-way ANOVA followed by *post hoc* Tukey's test.

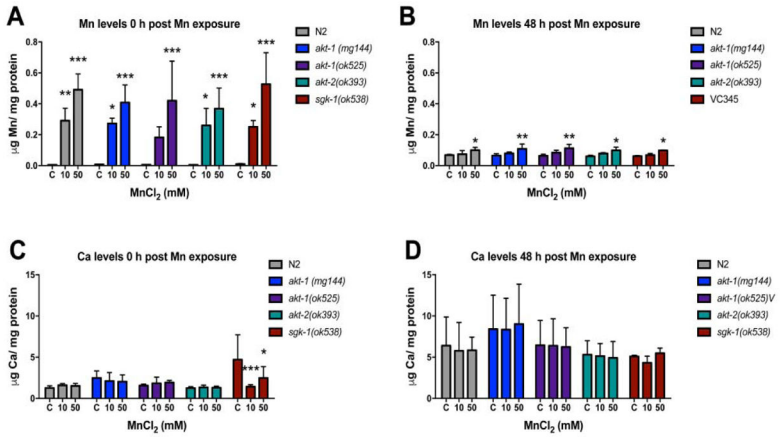

Fig. 2.

Intraworm manganese (A – B) or calcium (C – D) content after 1 h treatment with 10 or 50 mM $MnCl_2$ was quantified by ICP-MS immediately after treatment (0 h) or 48 h after. Metal content is expressed as µg/mg protein. Data are expressed as mean ± S.E.M. from three independent experiments. Statistical analysis by two-way ANOVA followed by *post hoc* Tukey's test. *$p < 0.05$, **$p < 0.01$, ***$p < 0.001$ compared to same strain control.

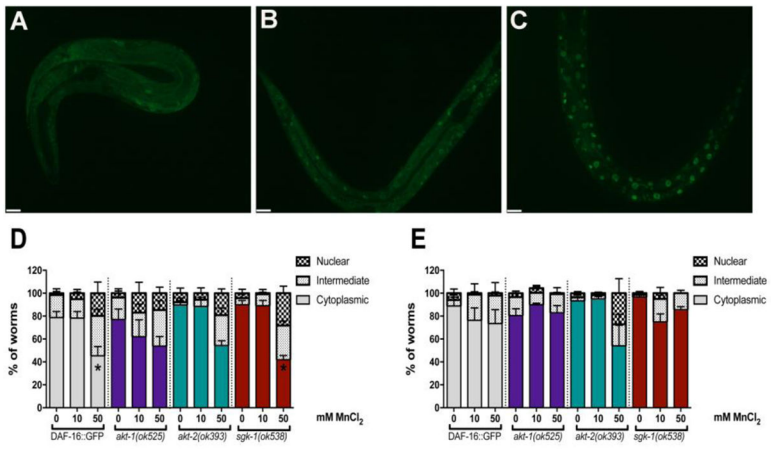

Fig. 3.

Mn induces DAF-16 nuclear translocation. *Akt-1(ok525)*, *akt-2(ok593)*, *sgk-1(ok538)* were crossed with *Pdaf-16A::GFP*. Worms were exposed to 10 or 50 mM $MnCl_2$ for 1 h. Controls were incubated with 85 mM NaCl. Worms were scored as having cytoplasmic (A), intermediate (B) or nuclear (C) DAF-16 distribution. DAF-16 was visualized by fluorescent microscopy within 10 min of Mn exposure (D), or at the end of 1 h exposure (E). Results are expressed as percent of worms with each condition. Data are expressed as mean + S.E.M. from five independent experiments. Statistical analysis by two-way ANOVA followed by *post hoc* Tukey's test. Representative images were obtained with a PerkinElmer spinning disk confocal, 40X objective. Scale bar represents 10μm.

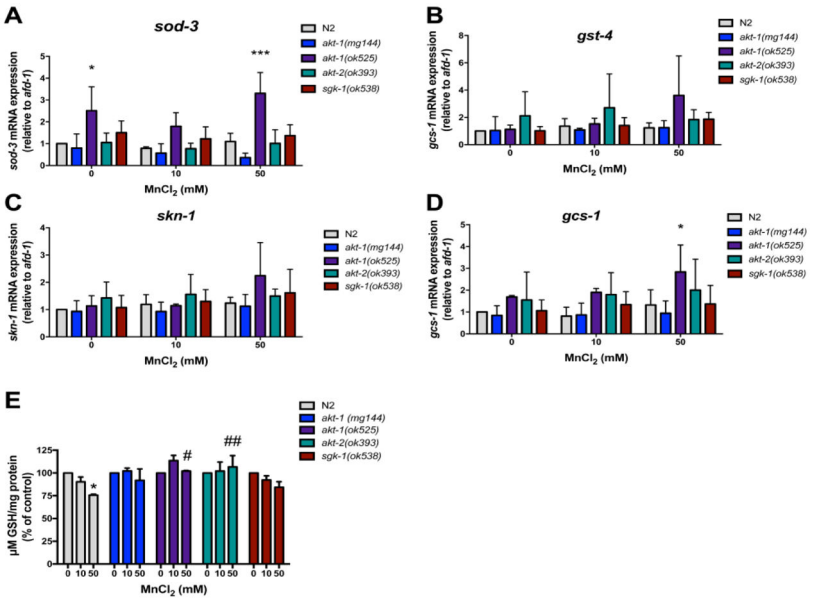

Fig. 4.

N2 (WT) or null mutants *akt-1(ok525)*, *akt-2(ok593)*, *sgk-1(ok538)* or gain-of-function mutant *akt-1(mg144)* were exposed to Mn for 1 h (10 or 50 mM). Controls were incubated with 85 mM NaCl. The worms were homogenized after treatment. Expression of *sod-3* (A), *gst-4* (B), *skn-1* (C) and *gcs-1* (D) relative to the constitutive gene *afd-1* (β-actin) was normalized to the N2 control group. Results are expressed as mean ± S.E.M. of 3 to 4 experiments. (E) GSH levels were determined using a standard curve (µM GSH/mg protein). Results are expressed as percentage GSH content relative to same strain control and mean ± S.E.M. of 3 experiments. * p <0.05, ** p <0.01, *** p <0.001 compared to the N2 control group. # p <0.05, ## p <0.01 compared to group 50 mM N2. Two-way ANOVA followed by *post hoc* Tukey's test.

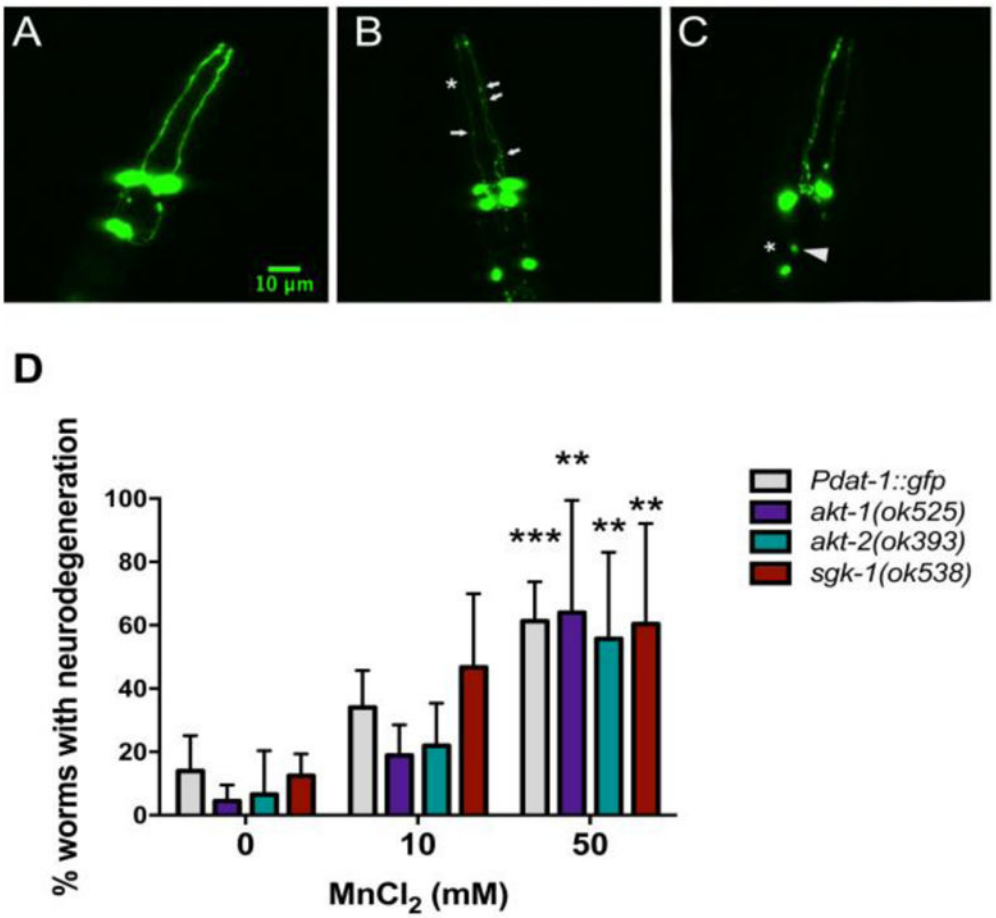

Fig. 5.

Morphology of CEPs and ADEs neurons DAergic neurons. Worms were evaluated 2 h after an acute treatment with $MnCl_2$ (10 or 50 mM) by fluorescence microscopy (X 40 magnification). Controls were incubated with 85 mM NaCl. Worms with healthy neurons were scored as normal (A). Worms with any of the following changes in their dopaminergic neurons were quantified as containing degeneration: (B) puncta (discontinuous marking the dendrite, arrows), (C) loss or cell body shrinkage (arrowhead), loss of dendrites (asterisks), exemplified in the confocal images. (D) Data represent the percentage of worms with degeneration. Results are expressed as mean ± S.E.M. of 6 experiments. * P <0.05, *** p <0.001 compared to the control group. Two-way ANOVA followed by *post hoc* Tukey's test. Representative images were obtained with a PerkinElmer spinning disk confocal, 40X objective. Scale bar represents 10 µm.

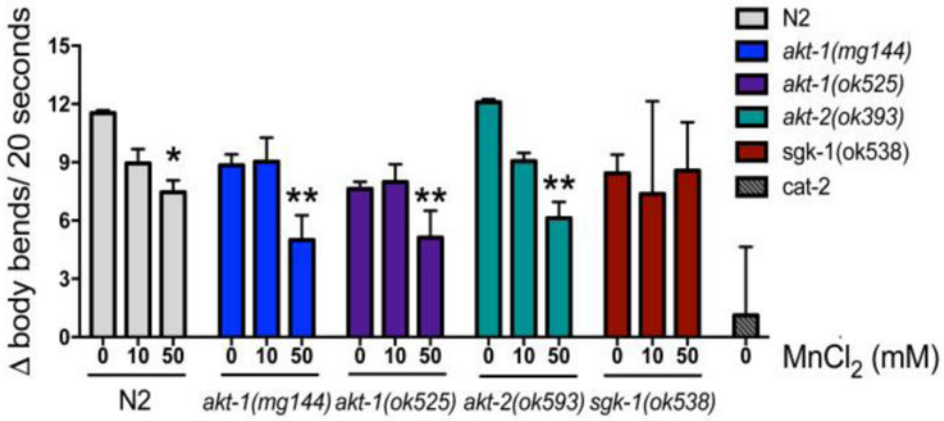

Fig. 6.

Basal slowing response was evaluated in WT N2 and null mutants *akt-1(ok525)*, *akt-2(ok593)*, *sgk-1(ok538)* and gain of function mutant *akt-1(mg144)* exposed to Mn for 1 h (10 or 50 mM). Controls were incubated with 85 mM NaCl. The test was performed 48 h after Mn exposure. Worms were washed off plates with S-basal and 5 worms were pipetted in plates with or without OP-50 *E.coli* (food). Worms were allowed to acclimate to the new plates for 5 min and then body bends were counted in 20 s intervals for each worm to obtain an average. Basal slowing response is expressed as number of body bends off food minus the number of body bends on food (Δ). *Cat-2* mutants, with deficiency in tyrosine hydroxylase, were used as positive control. Data are expressed as mean ± S.E.M. of 3 to 5 experiments. * $P < 0.05$, ** $p < 0.01$, compared to the N2 control group. Two-way ANOVA followed by *post hoc* Tukey's test.

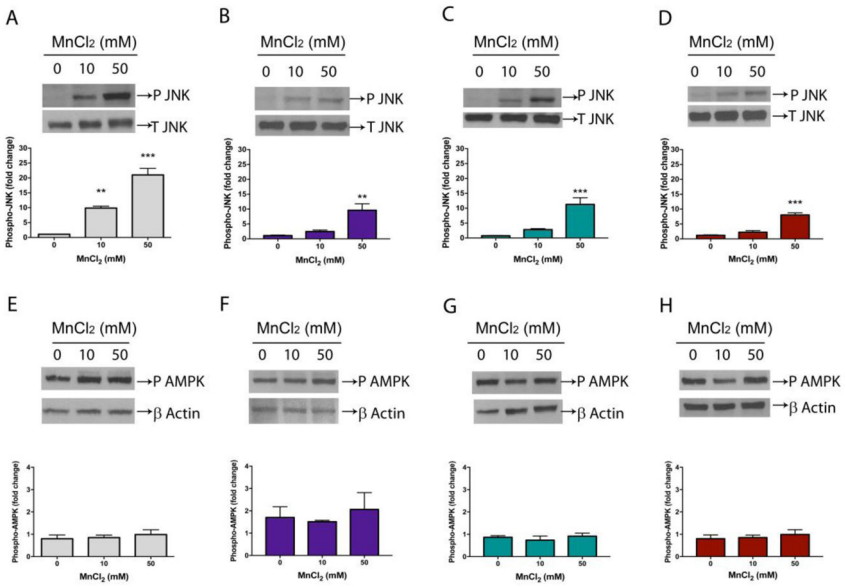

Fig. 7.

Phosphorylated proteins were evaluated by western blotting. Worms were exposed to Mn for 1 h (10 or 50 mM). Samples for SDS-PAGE were prepared immediately after treatment. Blots were developed by chemiluminescence. Bands were quantified by densitometry with imageJ software. (A) Phosphorylation of JNK in wild-type N2 or null mutants (B) *akt-1(ok525)*, (C) *akt-2(ok593)*, (D) *sgk-1(ok538).* Phosphorylated (P) JNK was normalized to total (T) JNK. (E) Phosphorylation of AAK/AMPK in wild-type N2 or null mutants (F) *akt-1(ok525)*, (G) *akt-2(ok593)*, (H) *sgk-1(ok538).* P AMPK was normalized to β-actin. Data represent fold change compared to controls and express the mean ± S.E.M. of 4 experiments. ** $p < 0.01$, *** $p < 0.001$ compared to controls (one-way ANOVA followed by *post hoc* Tukey's test).

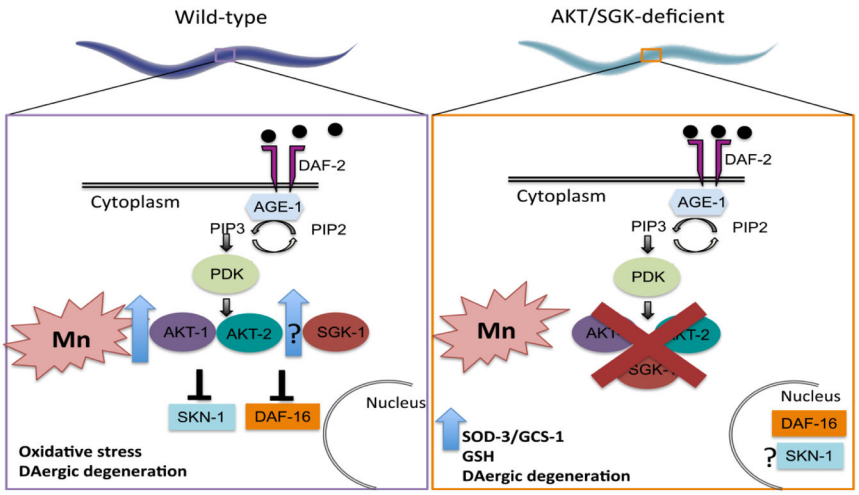

Figure 8.

Schematic representation of our findings. Previous work by our group reported increased AKT levels in worms exposed to Mn (Avila et al., 2012). Upstream of AKT-1/2 and SGK-1 is DAF-2 (the only receptor similar to mammalian insulin-like growth factor 1, IGF-1, receptor), activated by insulin-like peptides. DAF-2 activates AGE-1 (homologous of phosphatidyl inositol-3 kinase, PI3K), which converts phosphatidyl inositol-2 phosphate (PIP2) to PIP3 and activates phosphatidyl inositol-dependent kinase (PDK-1). PDK-1 activates AKT-1/2 and SGK-1, which in turn phosphorylate SKN-1 and DAF-16 at various sites, retaining the transcription factors in the cytoplasm. Our data indicate that AKT participates in Mn toxicity by preventing DAF-16 translocation to the nucleus. In AKT deficient mutants, we see increased DAF-16 nuclear localization (Fig. 3) and increased gcs-1 and sod-3 mRNA, which are DAF-16 targets (Fig. 4). This antioxidant response may be responsible for increased resistance to Mn exposure (Fig. 1) in mutant strains. This resistance is not observed in worm dopaminergic neurons. SGK-1 levels as well as SKN-1 nuclear translocation remain to be tested.